JOURNAL OF MATERIALS SCIENCE 31 (1996) 625–631

Microstructural evolution of a cold-deformed 6061Al reinforced with SiC particles during subsequent annealing

D. YU, P.R. MUNROE, S. BANDYOPADHYAY
School of Materials Science and Engineering, University of New South Wales, Sydney, NSW 2052, Australia

A. P. MOURITZ
Aeronautical and Maritime Research Laboratory, DSTO, P.O. Box 4331, Melbourne Victoria 3001, Australia

The microstructural development during annealing of a cold-deformed 6061Al metal matrix composite (MMC) reinforced with either 3 or 20 μm diameter SiC particles has been investigated. The composites were compressed to low (< 10%) levels of strain and then annealed at either 350 or 450 °C for different times. Microstructure examination was carried out by transmission electron microscopy and optical microscopy. The results reveal that prior grain boundaries and constituent particles are the dominant sites for recrystallization in both composites, although some nucleation was observed adjacent to the larger SiC particles. The concurrent presence of Mg_2Si precipitates affected the progress of recrystallization.

1. Introduction

Particulate reinforced aluminium metal matrix composites (Al MMCs) are very attractive for extensive industrial applications, such as aerospace and automotive industries, because of their low cost, low density, high stiffness and high strength [1, 2]. One of the advantages of these materials is that they can be processed and shaped by conventional metal working techniques, such as extrusion and rolling, due to their near isotropic properties. After such forming operations, most Al MMCs need to be heat treated to remove the effects of work hardening and restore ductility. Also, those Al MMCs with a precipitation hardening matrix may be solution treated and aged. Recent studies [3–8] have examined the development of microstructure in Al MMCs during such deformation and heat treatment. These studies report that the reinforcing particles have a significant influence on the deformation and recrystallization behaviour of the matrix alloy. First, the presence of ceramic particulates results in a more inhomogeneous microstructure in the matrix of MMCs after deformation compared with those unreinforced materials. Second, the recrystallization rate of MMCs is usually faster than in the equivalent unreinforced alloy. This enhanced rate of recrystallization is attributed to particle stimulated nucleation (PSN) where nucleation of new, strain-free grains occurs in the matrix adjacent to the reinforcement particle where regions of high strain exist.

However, the above studies have examined the recrystallization behaviour of MMCs deformed by large amounts of cold work (> 30%) which lead to PSN dominating the recrystallization processes. Also, most of the Al MMCs used in these studies have a pure Al matrix, while little work [5, 8] has been done on such behaviour of the MMCs based on heat treatable Al alloys, such as 6061, 2014 or 7075, which have been frequently used for commercial applications.

The work presented in this study examines the effect of presence of both large and small particles on the recrystallization behaviour of MMCs following small amounts, i.e. < 10% reduction, of deformation in two aluminium based composites (heat treatable 6061Al) reinforced with either 3 or 20 μm diameter SiC particulates at two different strain levels and two annealing temperatures. Some preliminary results on this research were reported earlier [9].

2. Experimental procedure

The composites used in this study were an aluminium alloy 6061 reinforced with (a) 3μm SiC particulates (referred to in this paper as composite A) and (b) 20 μm SiC particulates (composite B). Both

0022–2461

composites had a SiC volume fraction, V_f, of 20% and were manufactured through a powder metallurgy route. The unreinforced 6061 was also used as a reference material. After processing, all materials were heat treated to the T6 condition, i.e. solution treatment at 530 °C for 1.5 h, quenched in cold water, aged at room temperature for 20 h, and then artificially aged at 175 °C for 8 h. Details of the processing and heat treatment routes have been given elsewhere [9].

Uniaxial compression was performed using cylindrical specimens with diameter of 13 mm and length of 25 mm, compressed at room temperature at a strain rate of $8.3 \times 10^{-4}\,s^{-1}$ to a strain of either 6 or 9%. The specimens were deformed parallel to their original extrusion direction. After deformation, specimens were isothermally annealed at either 350 or 450 °C for times up to 7200 min, then immediately water quenched. Undeformed specimens of these materials were heat treated via the same route as deformed specimens, because the effect of the coarsening of precipitates (Mg_2Si) in the matrix (6061) must be considered. Vickers macrohardness measurements were carried out on the polished longitudinal section of both deformed and undeformed specimens following annealing using 5 kg load.

The microstructures of both the deformed and the annealed samples were studied by optical and transmission electron microscopy (TEM). Specimens for optical metallography were prepared using standard techniques. Thin foils for TEM were either jet polished or ion milled. Details of specimen preparation have been described elsewhere [9, 10]. The foils were examined in a JEOL 2000FX TEM.

3. Results and discussion

3.1. Initial and deformed microstructure

The initial microstructures of the unreinforced material and the two composites heat treated to the T6 condition have been described in detail elsewhere [9]. In brief, optical metallography revealed that the average grain size of the unreinforced material was 103 μm, while composite A exhibited a grain size of 4 μm and composite B a grain size of 7 μm. The shapes of the grains in both composites were more equiaxed than that in the unreinforced alloy and finer grains were observed in the vicinity of SiC particle clusters.

Further insight into the initial microstructure of the materials was provided by TEM. Representative matrix microstructures are shown in Fig. 1a, b for composite A and composite B, respectively. It can be seen that the length of needle-like precipitates β″ in composite B are about 50–70 nm, which is longer than those in composite A (about 20–40 nm). The size and distribution of precipitates in the monolithic alloy are similar to those in composite A. In addition to the needle-shaped β″ precipitates, there are some coarser particles (as indicated by arrow X in Fig. 1b) in all three materials and the size of such particles varies from ~0.1 to 1 μm. Energy dispersive spectrometry (EDX) analysis indicated [10] that they were probably

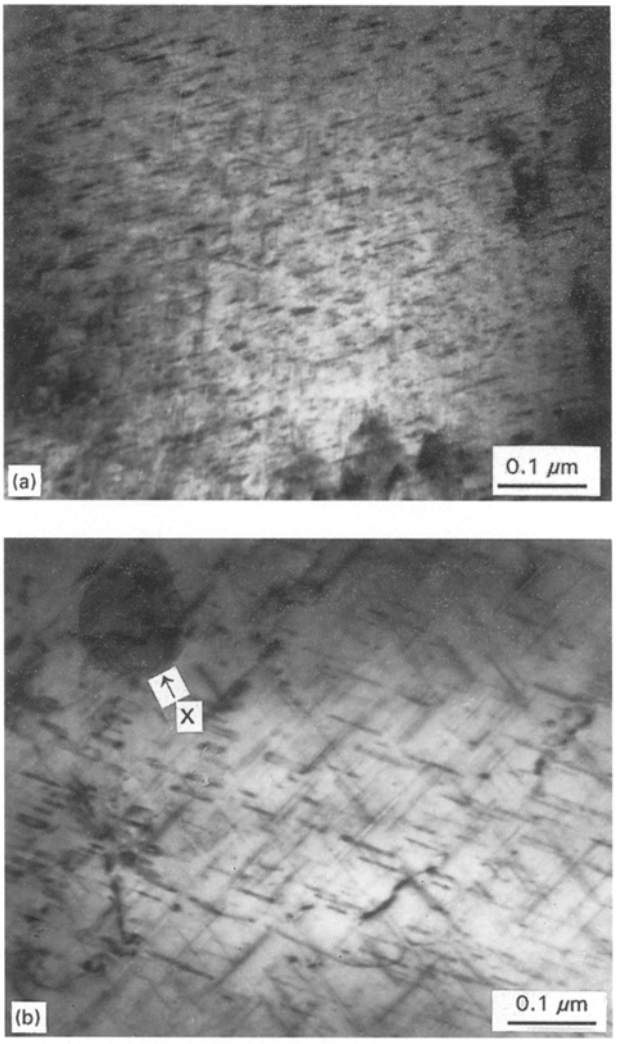

Figure 1 Bright field TEM micrographs showing needle-like precipitates of β″ phase in (a) composite A, and (b) composite B in the T6 condition.

$(Fe,Cr)_3SiAl_{12}$, which is a commonly observed intermetallic phase in wrought 6061 [11].

TEM studies showed that, following compression to a strain of either 6 or 9%, composite A exhibited a uniform deformation microstructure. A homogeneous array of dislocation tangles was observed within the grain (Fig. 2a). No enhanced deformation was observed in the vicinity of the SiC particles.

In contrast, the deformation microstructure of composite B showed some heterogeneities. In some regions of the aluminium matrix a cell-like structure was observed, with a cell diameter of about 0.1–0.2 μm (Fig. 2b). Also, some enhanced deformation zones were found in matrix regions adjacent to some SiC particles. However, these inhomogeneous microstructures were only observed in those samples which were deformed to a strain of 9%.

For the unreinforced 6061 alloy, the principal feature of the deformation microstructures were ill-defined cell structures (Fig. 2c) following compression to strains of both 6 and 9%.

3.2. Softening behaviour

In order to investigate the effect of deformation on the annealing behaviour of these materials, the specimens

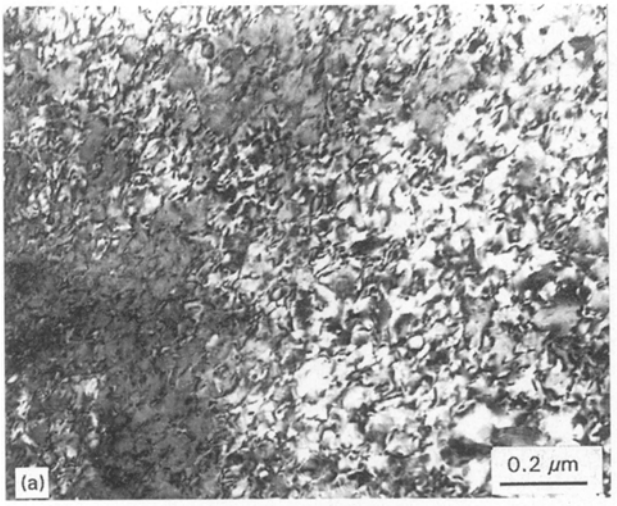

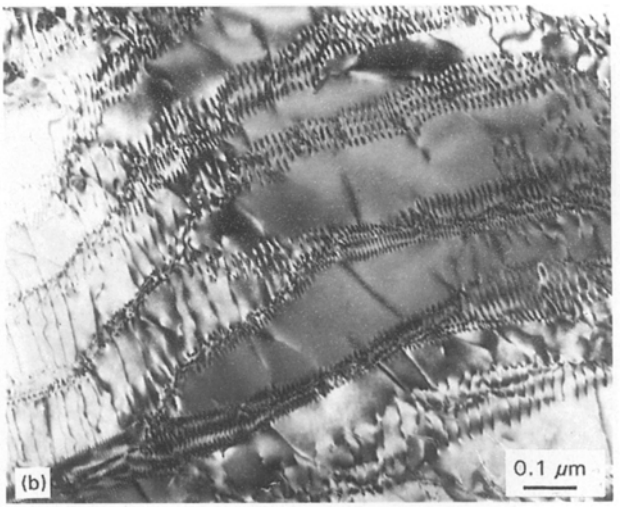

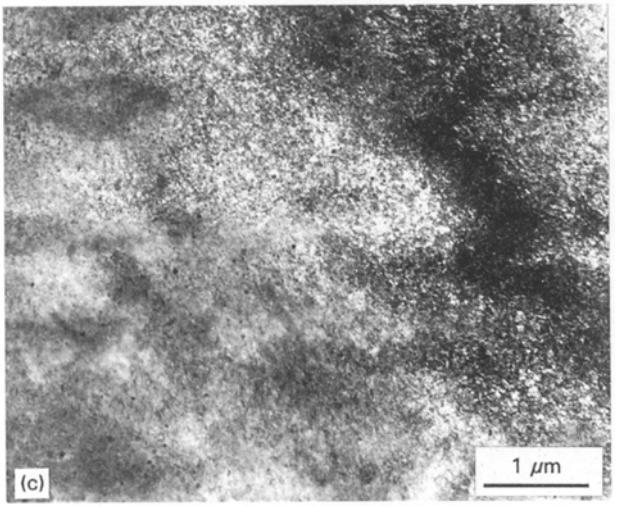

Figure 2 TEM micrographs showing representative microstructures of deformation in (a) composite A, (b) composite B, and (c) the 6061 alloy.

after both 6 and 9% deformation were annealed at 350 and 450 °C for various times. As seen in Fig. 3, following annealing at 350 °C, the hardness is seen to decrease slightly with increasing annealing time up to 1 min, after which it decreased rapidly up to times of about 10 min. However, the rate of softening is approximately the same for both composites and is independent of strains. For composite A, this is reasonable because there was no significant difference between the deformation microstructures after both 6 and 9% deformation. However, for composite B, some deformation zones in the vicinity of SiC particles were observed in the samples deformed at a strain of 9%. This suggests that such regions do not have a significant effect on the restoration behaviour, at these low strains. Fig. 3 shows that for both composites, softening occurred more rapidly following annealing at 450 °C and the hardness reached the minimum after about 5 min. Furthermore, both composites reach lower levels of hardness at the higher annealing temperature. Clearly, since restoration is a thermally activated process, the rate of restoration will increase with increasing annealing temperature. However, it is worth noting that during annealing softening occurs not only through restorative processes but also through precipitate coarsening in the matrix. Therefore, at 450 °C, the lower hardness may also be attributed to the formation of more coarser precipitates β-Mg_2Si. More details on the development of microstructures during annealing are given in the next section.

3.3. Microstructural development during annealing

Both optical microscopy and TEM studies performed on the monolithic alloy revealed that recrystallization

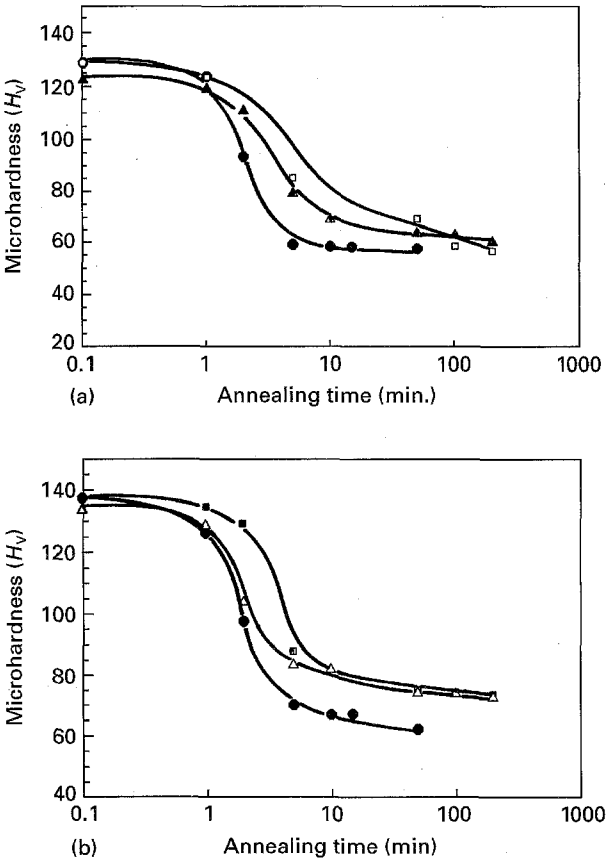

Figure 3 Softening behaviour of (a) composite A and (b) composite B after either 6% deformation at 350 °C (▲, △) or 9% deformation at 350 °C (■, □) and 450 °C (●).

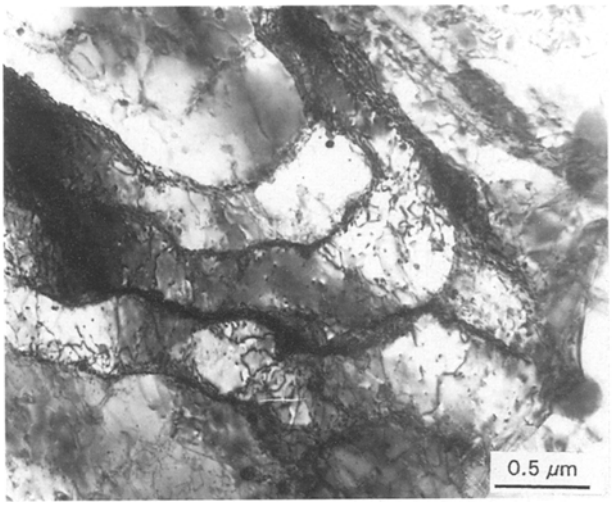

Figure 4 TEM micrographs showing recovery in unreinforced 6061 alloys following 9% strain in compression after 10 min at 350 °C.

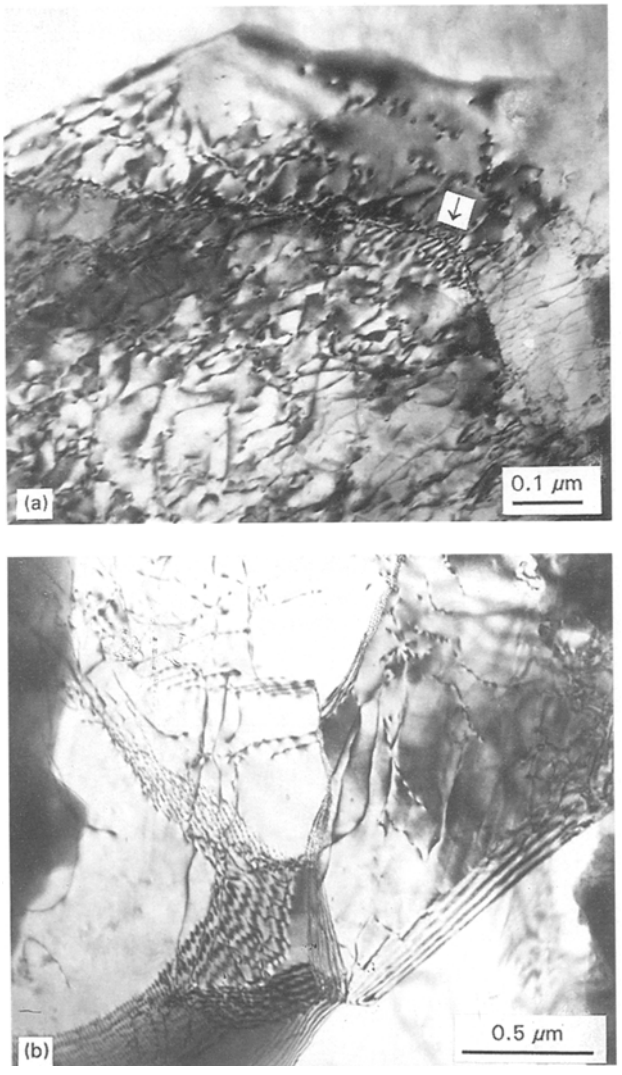

Figure 5 TEM micrographs showing the dislocation rearrangement in composite A after 9% compression during annealing at 350 °C for (a) 1 min, and (b) 50 min.

did not occur during annealing at 350 °C, even after prolonged periods (7200 min). However, subgrain formation indicative of recovery was observed in the microstructure (Fig. 4). It is clear that in this material,

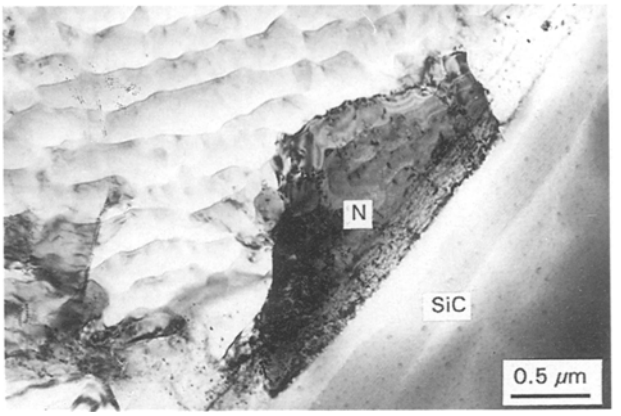

Figure 6 TEM micrographs of typical nucleation sites in the vicinity of a SiC particle in composite B after annealing at 350 °C.

there was insufficient deformation to provide regions of high strain gradients and lattice misorientation necessary to induce the nucleation of new grains.

For both composites after 9% compression and subsequent annealing at 350 °C, a rapid drop in hardness occurred between 2 and 5 min annealing time. Prior studies [9] have shown that hardness of undeformed samples did not drop significantly during the first 5 min of annealing at the same temperature, so it would suggest that the enhanced rate of softening was attributable to microstructural restoration having taken place in these composites. However, TEM examination of both composites showed that the overall restoration process was dominated by recovery, and recrystallization nuclei were not observed until after annealing for 50 min. During the early stages of annealing (about 1–2 min), subgrain formation (arrowed in Fig. 5a) occurred, but this behaviour was localized and the dislocation density was still high and relatively uniform in some regions. After annealing at 350 °C for 50 min the dislocation density in both composites decreased and well defined subgrain formation was dominant (Fig. 5b). However, in neither composite was enhanced recovery observed in the matrix in the vicinity of SiC particles.

Previous TEM studies of these materials [9] revealed evidence of recrystallization in both composites following an annealing time of 50 min at 350 °C. In both materials recrystallization nuclei were found to form preferentially at prior grain boundaries and often in the vicinity of constituent particles. In addition, a small number of nuclei were also observed adjacent to SiC particles in composite B (see Fig. 6), but not in composite A. This may be due to the fact that the deformation microstructure of composite A was relatively homogeneous and the particle size (3 μm) was

TABLE I Mean subgrain size (μm) after deformation and after annealing at 350 °C

Materials	As-deformed (9%)	50 min	200 min
Composite A	–	0.89	1.14
Composite B	0.2	0.97	1.15

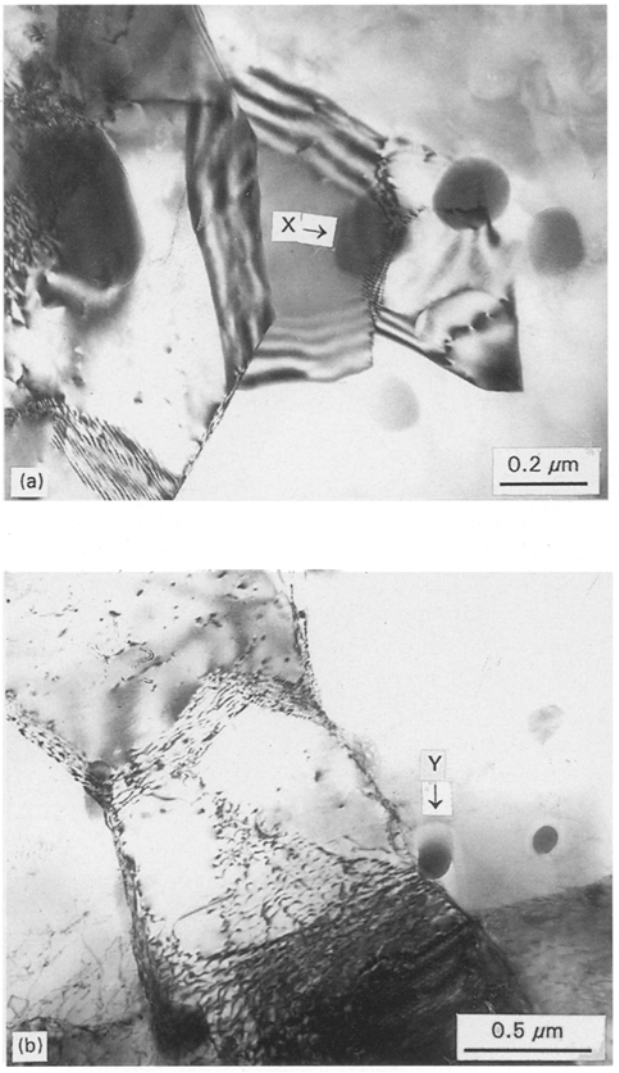

Figure 7 Bright field TEM micrographs showing the precipitate particles (arrowed at X and Y) associated with low angle grain boundaries in (a) composite A and (b) composite B. Both specimens had been annealed for 50 min at 350 °C after 9% compression.

too small to lead to the formation of localized deformation zones which in turn would lead to nucleation in these regions. Although some PSN was evident in composite B, the prior grain boundaries were still the dominant site for nucleation. Compared with the unreinforced 6061 alloy, both composites have a much smaller initial grain size. This means that the density of grain boundaries in the composites was much higher than that in monolithic alloy. As a consequence, both composites have more potential nucleation sites than the monolithic alloy, which is reflected in the occurrence of recrystallization nuclei in the composites but not in the monolithic alloy.

The subgrain sizes of both composites after annealing at 350 °C up to 200 min are given in Table I. The cell size of the as-deformed composite B is also included for comparison. However, due to the homogeneous deformation microstructure of composite A, such data were not measurable in this material.

It can be seen that there is an increase in subgrain sizes for both composites during the first 50 min of annealing. However, after further annealing from 50 to 200 min, the subgrain growth was very slow and both composites exhibited almost the same average subgrain size. Liu *et al.* [12, 13] recently studied the recovery in MMCs, where they noted that the presence of small oxide particles (< 50 nm diameter) retarded the subgrain growth in a composite containing 2 vol % SiC_w as the reinforcement. Such retardation was due to these small particles pinning dislocations and subgrain boundaries. In the present study, a low density of Mg_2Si particles (about 200 nm in diameter) was found to interact with and pin the subgrain boundaries (as shown in Fig. 7). However, extensive subgrain–particle interactions were not observed. It is more likely that in these materials, such a slower rate of subgrain growth is due to the lower stored energy in these materials after small amounts of deformation.

Following annealing at 450 °C, both composites exhibited a faster rate of softening compared with annealing at 350 °C (Fig. 3). TEM examination showed that the nuclei were observed after annealing at 450 °C for only 10 min (Fig. 8a) and recovery also occurred more rapidly (Fig. 8b). Furthermore, some nuclei were found adjacent to SiC particles only in composite B (Fig. 8c) but not in composite A, although the prior grain boundaries and constituent particles were dominant sites for nucleation. It is also noticed that, after annealing for 50 min at 450 °C, the size of precipitates was much smaller than when annealed at 350 °C for the same time (Fig. 8d; compare with Fig. 7b). However, larger Mg_2Si was observed at the high angle grain boundary (arrowed by × in Fig. 8d). This indicated that at this stage some of the β′ precipitates in the matrix dissolved to form much coarser equilibrium Mg_2Si. This may have enhanced dislocation mobility and thus enhanced the rate of recovery. Simultaneously, the precipitates which have been at the grain boundaries also coarsened quickly due to accelerated diffusion at grain boundaries [14]. These coarser precipitates may have been more efficient in pinning the grain boundary so the grain growth was probably more retarded.

4. Conclusions

Following low compressive strains (< 10%), some differences were observed in the deformation microstructure of the two composites, i.e. the deformation zones were more likely to form around the larger SiC particles. Although some nucleation was observed near larger SiC particles in composite A during annealing, prior grain boundaries and constituent particles are the dominant sites for recrystallization for both composites A and B. The present study shows that, despite the insufficient driving force for the growth of nuclei due to lower degrees of deformation, the coarser precipitates and their formation during annealing also retarded the progress of recrystallization. However, such effects are very complex and further study is required.

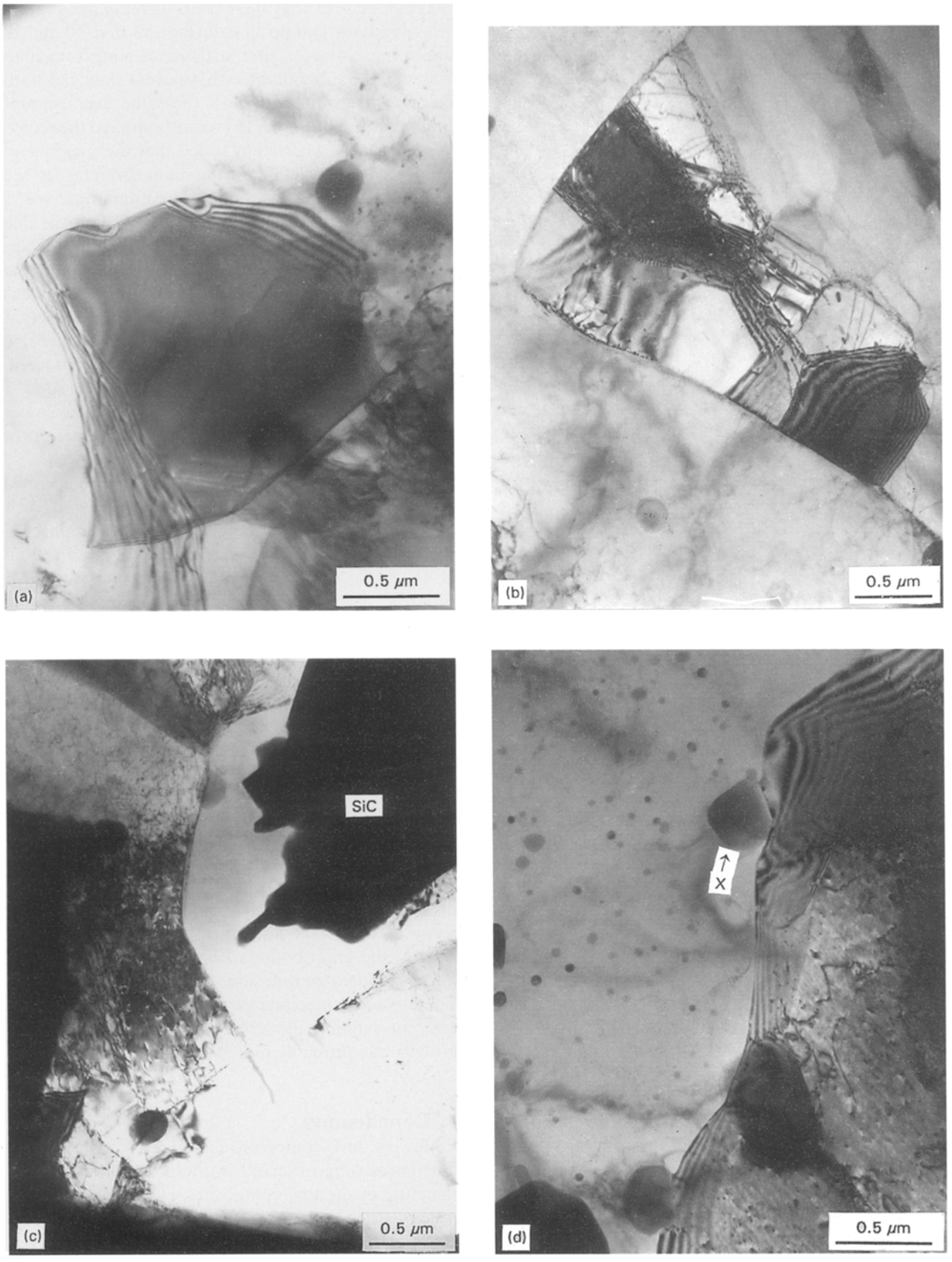

Figure 8 TEM micrographs showing features in 9% deformed composite B after annealing at 450 °C for (a) 10 min, (b) 10 min, (c) 5 min, and (d) 50 min.

References

1. I. A. IBRAHIM, F. A. MOHAMED and F. J. LAVERNIA, *J. Mater. Sci.* **26** (1991) 1137.
2. D. J. LLOYD, *Inter. Mater. Rev.* **39** (1994) 1.
3. F. J. HUMPHREYS, W. S. MILLER and M. R. DJAZEB, *Mater. Sci. Technol.* **6** (1990) 1157.
4. R. A. SHAHANI and T. M. CLYNE, *Mater. Sci. Eng.* **A135** (1991) 285.
5. M. FERRY, P. R. MUNROE, A. CROSKY and T. CHANDRA, *ibid.* **8** (1992) 43.

6. Y. L. LIU, N. HANSEN and D. J. JENSEN, *Met. Trans.* **20A** (1989) 1743.
7. *Idem, Mater. Sci. Technol.* **7** (1991) 270.
8. T. CHANDRA and D. YU, *Mater. Forum* **15** (1991) 343.
9. D. YU, P. R. MUNROE, S. BANDYOPADHYAY and A. P. MOURITZ, *Scripta Metall. Mater.* **30** (1994) 927.
10. D. YU, M.Sc thesis, The University of New South Wales (1994).
11. Metals Handbook, Vol. 9, 9th Edn (American Society for Metals, Metals Park, OH, 1985).
12. Y. L. LIU, D. J. JENSEN and N. HANSEN, *Met. Trans.* **23A** (1992) 807.
13. *Idem, Mater. Sci. Forum* **113–115** (1993) 539.
14. R. D. DOHERTY and J. W. MARTIN, *Trans. ASM* **57** (1964) 874.

Received 25 October 1994
and accepted 7 June 1995